Journal of Colloid and Interface Science 393 (2013) 314–318

Contents lists available at SciVerse ScienceDirect

Journal of Colloid and Interface Science

www.elsevier.com/locate/jcis

Complexation at the edges of hydrotalcite: The cases of arsenate and chromate

Matías Jobbágy [a], Alberto E. Regazzoni [b,c,*]

[a] INQUIMAE, Facultad de Ciencias Exactas y Naturales, Universidad de Buenos Aires, Pabellón II, Ciudad Universitaria, C1428EHA-Buenos Aires, Argentina
[b] Gerencia Química, Centro Atómico Constituyentes, Comisión Nacional de Energía Atómica, Av. General Paz 1499, B1650KNA-San Martín, Argentina
[c] Instituto de Tecnología Jorge A. Sabato, Universidad Nacional de General San Martín, Av. General Paz 1499, B1650KNA-San Martín, Argentina

ARTICLE INFO

Article history:
Received 15 September 2012
Accepted 29 October 2012
Available online 8 November 2012

Keywords:
Layered double hydroxides
Hydrotalcite
Arsenate
Chromate
Adsorption
Surface complexation

ABSTRACT

Sorption of CrO_4^{2-} and $HAsO_4^{2-}$ by hydrotalcite, in its chloride form, was studied as a function of anion concentration. In both cases, the shape of the isotherms is langmuirian. The maximum uptake of CrO_4^{2-} equals the ion-exchange capacity of the solid, whereas sorption of $HAsO_4^{2-}$ saturates at a higher value. Chloride ions inhibit the uptake of both anions, the amount of sorbed CrO_4^{2-} declining rapidly to zero. The uptake of $HAsO_4^{2-}$, however, attains a constant value at high chloride concentrations. The excess of arsenate uptake follows, at constant pH, a langmuirian dependence with equilibrium concentration and decreases with increasing pH, depicting a marked change in slope at $pH \approx pQ_{a3}$. CrO_4^{2-} and $HAsO_4^{2-}$ have notable, albeit different, effects on the electrophoretic behavior of hydrotalcite; the positive particle charge is screened almost completely by CrO_4^{2-}, whereas sorption of $HAsO_4^{2-}$ produces charge reversal. These results reflect the formation of inner-sphere arsenate surface complexes at the edges of hydrotalcite particles. The underlying rationale is discussed in terms of the crystal structure of hydrotalcite surfaces.

1. Introduction

Layered double hydroxides (LDHs) are stacks of hexagonal $M(OH)_2$ layers containing divalent and trivalent metal ions in mole ratios that span typically from 2 to 4. These slabs are held together by intercalated anions, which counterbalance their excess positive charge and determine the basal spacing of the solid [1]; water molecules, as well, occupy the interlamellar space. Whereas natural LDHs are rather scarce, the variety of synthetic LDHs is nowadays huge [2,3]. Small inorganic interlamellar anions, except carbonate, are readily exchangeable [4]. For this reason, these materials are regarded as promising sorbents for the removal of dissolved toxic anions [5–11]. Anion uptake is dominated by ion-exchange; thus, maximum uptake capacities are determined by the composition of the brucite-like layers (i.e., by their M(II)/M(III) mole ratios) and by the charge number of the incoming anion. Affinities, on the other hand, are influenced by anion charge/size ratios [12], as well as by enthalpic and entropic contributions [13,14].

Clearly, anion exchange is a phenomenon that involves the bulk of LDHs. However, it has been recently suggested that adsorption at the edges of LDHs particles may also be of importance. Wang and Gao [15], based on structural considerations, argued that sorption at edges is driven by a *cage effect*; according to them, the interlaminar space and the voids between corner-sharing $M(OH)_6$ octahedra at edges of the brucite-like layers define a cage, which should provide a suitable sorption chemical environment for fitting anions. On the other hand, Goh et al. [16], based on the ideas set by the well-known surface complexation approach [17–19], suggested that oxyanions form also inner-sphere complexes at the edges of hydrotalcite. Despite the latter suggestion is indeed sound, the evidence advanced by the authors is rather feeble.

Aiming at assessing the actual role of the edges of LDHs particles in the uptake of oxyanions, this work presents a detailed study of the effect of chloride concentration on the sorption of arsenate and chromate by Cl-hydrotalcite and reports the electrophoretic behavior Cl-hydrotalcite immersed in arsenate and chromate aqueous solutions.

2. Experimental

Chloride-hydrotalcite was synthesized by coprecipitation as described previously [20]. The so-prepared solid is composed of ca. 100 nm size hexagonal platelets. Its XRD pattern depicts reflections that are typical of LDHs, the basal spacing being 0.786(2) nm, and $d_{110} = 0.305(1)$ nm. Its chemical composition, which was assessed by elemental analyses, is given by the formulae $Mg_{0.73}Al_{0.27}(OH)_2Cl_{0.19}(CO_3)_{0.04}\cdot H_2O$.

Chromate and arsenate sorption experiments were performed as follows: weighted aliquots of a 4 g L^{-1} aqueous dispersion of

* Corresponding author at: Gerencia Química, Centro Atómico Constituyentes, Comisión Nacional de Energía Atómica, Av. General Paz 1499, B1650KNA-San Martín, Argentina. Fax: +54 11 6772 7886.
E-mail address: regazzon@cnea.gov.ar (A.E. Regazzoni).

0021-9797/$ - see front matter © 2012 Elsevier Inc. All rights reserved.
http://dx.doi.org/10.1016/j.jcis.2012.10.069

hydrotalcite were placed in Pyrex flasks, to which measured volumes of solutions containing K_2CrO_4 (or Na_2HAsO_4) and KCl in known concentrations were added. The pH of the resulting suspensions was measured and adjusted (when required) by adding a small volume of a KOH solution of appropriate concentration. The systems were then left to equilibrate under constant stirring for 1 h at room temperature (23 ± 1 °C); preliminary experiments showed that sorption equilibrium is attained in ca. 20 min. Afterward, the suspensions were filtered throughout 0.22 μm pore-size nitrocellulose membranes, and the supernatants stored for analyses. Chromate and arsenate concentrations were measured by ICP-AES in a Perkin Elmer Optima 5100 spectrometer. The amount of Cr(VI), or As(V), taken up per gram of hydrotalcite (q) was then determined solving the mass balance of the systems, that is,

$$q = \frac{(C_0 - C)V}{m} \quad (1)$$

where C_0 is the total Cr(VI), or As(V), concentration, C is the concentration of the equilibrated solution, V is the volume of the aqueous phase, and m is the mass of hydrotalcite in the system.

Electrophoretic mobility measurements were carried out using a Malvern Zeta Sizer 2000 apparatus. For this purpose, Cl-hydrotalcite particles were dispersed in 5×10^{-3} M KCl, 5×10^{-3} M K_2CrO_4, and 5×10^{-3} M Na_2HAsO_4 solutions of prefixed pH and let to equilibrate for at least 1 h before the measurements; all solutions were pre-filtered through 0.22 μm pore-size membranes. All suspensions were extremely diluted to avoid possible artifacts due to multiple scattering. Consequently, the concentrations of Cr(VI) and As(V) in equilibrium with the solid can be safely assumed to be equal to the total concentration of the salts. Measured electrophoretic mobility values were cast as zeta potential (ζ) using von Smoluchowski's equation. Despite these experiments were performed at a different ionic strength, the observed electrophoretic behaviors can be safely compared; in the studied range, the influence of ionic strength on ζ is negligible.

To avoid dissolution of the solid phase [21], all experiments were carried out at pH ⩾ 9.3, which is the natural pH of hydrotalcite aqueous suspensions; it is worth mentioning that dissolution may blur the interpretation of the data.

Analytical grade reagents and deionized water (18 MΩ cm^{-1}), obtained from an E-pure apparatus, were used in all experiments. They were performed under a CO_2-free nitrogen blanket to avoid carbonate contamination. pH values were measured using a combined glass electrode and a Metrohm 654 pH-meter.

3. Results and discussion

Figs. 1 and 2, which show respectively the sorption isotherms of CrO_4^{2-} and $HAsO_4^{2-}$ at pH 9.3, indicate that Cl-hydrotalcite sorbs both anions very efficiently. At this pH value, both chromate (pK_{a2} = 6.51) and arsenate (pK_{a2} = 6.96; pK_{a3} = 11.50) are present as dianions (see Supplementary data), thus the uptake of Cr(VI) and As(V) must be accounted for by the following anion exchange equilibria:

$$1/2CrO_4^{2-}(aq) + HTCl(s) = Cl^-(aq) + HT(CrO_4)_{1/2}(s) \quad (2)$$

$$1/2HAsO_4^{2-}(aq) + HTCl(s) = Cl^-(aq) + HT(HAsO_4)_{1/2}(s) \quad (3)$$

where HT stands for $[Mg_{3.84}Al_{1.42}(OH)_{10.52}(CO_3)_{0.21}]^+$; interlamellar water molecules were omitted. Note that carbonate ions are not exchangeable [4,20]

Both sorption profiles, however, can be well described by the Langmuir adsorption model, from which the parameters listed in Table 1 were derived; maximum uptake capacities, q_m, were determined from the reciprocal of the slopes of the straight lines (Eq. (4)) shown in the insets of Figs. 1 and 2. For anion exchange reactions (Eqs. (2) and (3)), compliance of the data presented in latter figures with the Langmuir adsorption model is fortuitous [20], thus the derived K_L values ought to be regarded as operational ones [22]. Nonetheless, Eq. (4) allows for the accurate determination of q_m, on which we shall center our attention.

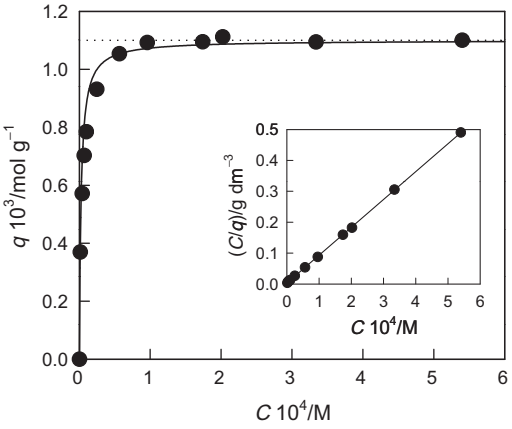

Fig. 1. Uptake of Cr(VI) as a function of the chromate equilibrium concentration; hydrotalcite load: 0.8 g L^{-1}; pH = 9.3 ± 0.1. The dotted line shows the value of the maximum exchange capacity. Inset: data re-plotted in terms of Eq. (4).

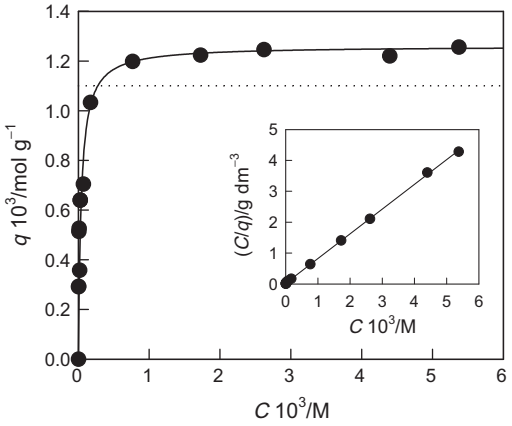

Fig. 2. Uptake of As(V) as a function of the arsenate equilibrium concentration; hydrotalcite load: 3.1 g L^{-1}; pH = 9.3 ± 0.1. The dotted line shows the value of the maximum exchange capacity. Inset: data re-plotted in terms of Eq. (4).

Table 1
Langmuirian parameters describing the uptake of chromate and arsenate by chloride-hydrotalcite.

Anion	K_L (M^{-1})	q_m (mmol g^{-1})	$q_m - mec_{1:2}$
CrO_4^{2-}	4.0×10^5	1.11	0
$HAsO_4^{2-}$	2.5×10^4	1.26	0.15

$$\frac{C}{q} = \frac{1}{q_m K_L} + \frac{1}{q_m} C \quad (4)$$

For chromate, the maximum uptake matches exactly $mec_{1:2}$, which is the value of the maximum exchange capacity that results from the chemical composition of the exchanger phase and the anticipated 1:2 anion exchange stoichiometry (Eq. (2)). For $HAsO_4^{2-}$, on the other hand, q_m is larger than $mec_{1:2}$. The excess, which is about 14%, cannot be attributed to a departure from the exchange stoichiometry. Deviations from the expected anion ex-

change stoichiometry are in fact possible; Ookubo et al. [4] have shown that intercalation enhanced the acidity of $H_2PO_4^-$ anions. However, if deprotonation of intercalated $HAsO_4^{2-}$ had occurred, the measured value of the maximum uptake of arsenate would have ranged between 0.74 and 1.11 mmol g^{-1} (i.e., $mec_{1:3} \leqslant q_m \leqslant mec_{1:2}$), but could not have surpassed the latter limit.

The uptakes of CrO_4^{2-} and $HAsO_4^{2-}$ by Cl-hydrotalcite are not only distinguished by their different saturation values, but also by their unlike responses toward KCl concentration (Figs. 3 and 4). As predicted by Eq. (2), $q_{Cr(VI)}$ declines rapidly to zero with increasing chloride concentration. On the contrary, $q_{As(V)}$ depicts a much slower decrease and attains a non-null, nearly constant, value at high chloride concentrations. Undoubtedly, the uptake of chromate by Cl-hydrotalcite must be solely interpreted in terms of Eq. (2) and can be described by any suitable anion exchange formalism, as that presented elsewhere [20].

The evident excess of arsenate uptake indicates that an additional phenomenon, besides anion exchange, drives arsenate sorption. A *cage effect* at edges, as suggested by Wang and Gao [15], is difficult to conceive, because LDHs adapt their interlamellar spaces to accommodate a variety of incoming anions of different sizes [23–25]. Therefore, the origin of the observed supra-stoichiometric arsenate uptake (Table 1) and the inability of KCl to suppress the uptake of arsenate (Fig. 4) must be traced back to a more specific interaction, such as that visualized by Goh et al. [16]. Indeed, following the ideas introduced by the MUSIC model [26–28], inspection to the structure of the most probable faces of hydrotalcite crystals points toward chemisorption at the particle edges, that is, formation of inner-sphere complexes at the 100, 010, and other structurally equivalent surfaces.

Fig. 5 depicts the structure of the perfectly cleaved, fully hydrated, edges of a brucite-like sheet. There, two types of adsorption sites can be easily recognized. They are edge metal ions coordinated to one water molecule, and corner metal ions coordinated to two water molecules, the latter being the minority. Bi-coordinated OH groups bridging two adjacent edge metal ions can also be recognized at the edges. Since per every edge metal ion there is one bi-coordinated OH group and one mono-coordinated water molecule, edge adsorption sites can be represented as $\equiv Mg(OH)(OH_2)$ and $\equiv Al(OH)(OH_2)$.

Inner-sphere surface complexation is a ligand-exchange reaction [18,19]. Kinetically, it is determined by the lability of the OH surface groups; thus, bi-coordinated OH groups, which participate in protonation–deprotonation surface reactions, are not directly involved in chemisorption [29], at least within the time frame of typical sorption experiments; the rates of exchange of singly- and bi-coordinated OH groups are dramatically different [30]. By the same token, tri-coordinated OH groups, present at the 001 basal surfaces (Fig. 5), are inert toward ligand-exchange; hence, adsorption onto these surfaces is essentially electrostatic.

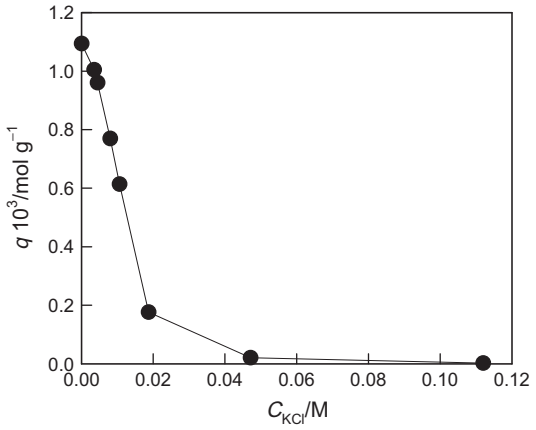

Fig. 3. Uptake of Cr(VI) as a function of the concentration of added KCl; total Cr(VI) concentration: 1.2×10^{-3} M; hydrotalcite load: 0.8 g L^{-1}; pH = 9.3 ± 0.1. The solid line is a guide to the eye.

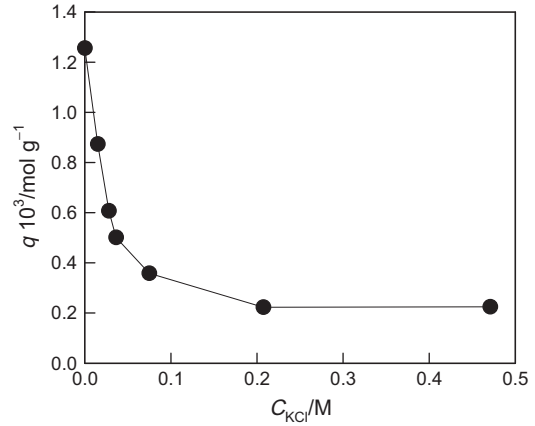

Fig. 4. Uptake of As(V) as a function of the concentration of added KCl; total As(V) concentration: 7.1×10^{-3} M; hydrotalcite load: 2.7 g L^{-1}; pH = 9.3 ± 0.1. The solid line is a guide to the eye.

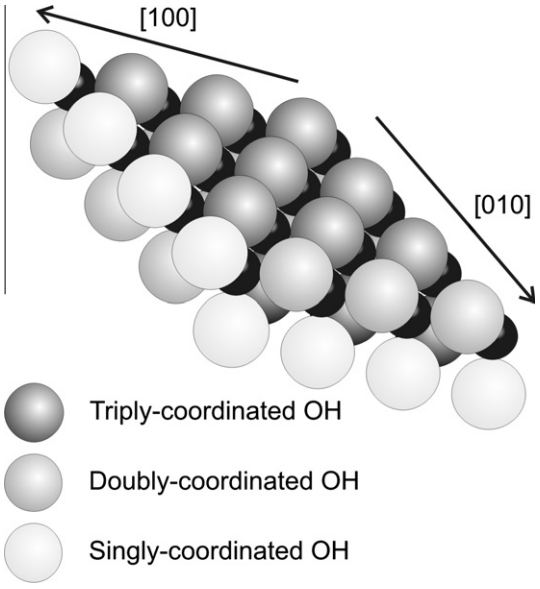

Fig. 5. Structure of the fully hydrated edges of hydrotalcite crystals.

Chemisorption of arsenate at the edges of hydrotalcite must, therefore, be accounted for by the following surface (edge) complexation equilibria,

$$\begin{matrix}\equiv Mg(OH)(OH_2)\\ \equiv Mg(OH)(OH_2)\end{matrix} + HAsO_4^{2-} \rightleftharpoons \begin{matrix}\equiv Mg(OH)O\\ \equiv Mg(OH)O\end{matrix}\rangle AsO(OH)^{2-} + 2H_2O \quad (5)$$

$$\begin{matrix}\equiv Al(OH)(OH_2)\\ \equiv Mg(OH)(OH_2)\end{matrix} + HAsO_4^{2-} \rightleftharpoons \begin{matrix}\equiv Al(OH)O\\ \equiv Mg(OH)O\end{matrix}\rangle AsO(OH)^{2-} + 2H_2O \quad (6)$$

the potential-dependent equilibrium quotients being given by the mass-action law, for example,

$$Q = \frac{\left\{\begin{matrix}\equiv Mg(OH)O\\ \equiv Mg(OH)O\end{matrix}\rangle AsO(OH)^{2-}\right\}}{\left\{\begin{matrix}\equiv Mg(OH)(OH_2)\\ \equiv Mg(OH)(OH_2)\end{matrix}\right\}[HAsO_4^{2-}]} \quad (7)$$

where {} represents surface (edge) concentration; an analogous equation can be written for equilibrium 6.

Arsenate edge complexes like those depicted in Eq. (5) have already been described in the literature [31]. Chromate anions may also form inner-sphere edge complexes [32], but the contribution of such complexes to the overall uptake of Cr(VI) by hydrotalcite is indisputably negligible (cf. Table 1 and Fig. 3). This reflects the much lower affinity of CrO_4^{2-} for the edge metal ions. The noted unlike behaviors of arsenate and chromate are in line with the stability trend discussed by Dzombak and Morel [17]; the more basic oxoanions chemisorb more strongly.

From the data in Figs. 3 and 4, it is reasonable to conclude that, under our experimental conditions, chloride ions in concentrations of the order of, say, 0.3 M, suppress anion exchange totally (cf. Eqs. (2) and (3)). Therefore, $q_{As(V)}$ quotients measured under such conditions represent As(V) edge excess values ($\Gamma_{As(V)}$); viz. the concentration of arsenate edge complexes (Eq. (8)). Fig. 6 shows that $\Gamma_{As(V)}$ increases with arsenate equilibrium concentration in a langmuirian fashion ($Q = 8.55 \times 10^3\ M^{-1}$ and $N_S = 0.25$ mmol g^{-1}). Interestingly, N_S is about twice $q_m - mec_{1:2}$ (cf. Table 1), which suggests that a fraction of arsenate might have been intercalated as AsO_4^{3-}, in the experiments portrayed by Fig. 2 (cf. Ref. [4]).

$$\Gamma_{As(V)} = \left\{ \begin{matrix} \equiv Al(OH)O \\ \equiv Mg(OH)O \end{matrix} \right\rangle AsO(OH)^{2-} \Bigg\} + \left\{ \begin{matrix} \equiv Mg(OH)O \\ \equiv Mg(OH)O \end{matrix} \right\rangle AsO(OH)^{2-} \Bigg\} \quad (8)$$

Whether the measured $\Gamma_{As(V)}$ values are determined by chemisorption onto aluminum–magnesium or magnesium–magnesium edge sites, depends on their relative abundance, which is fixed by the stoichiometry of the hydrotalcite. It also depends on the affinity of arsenate for magnesium and aluminum edge ions. Arsenate is known to interact strongly with the surface of aluminum oxides [33–35]; thus, it is conceivable that arsenate would form more stable complexes with aluminum–magnesium sites. Our data, however, are insufficient to distinguish the actual weight of the contributions to $\Gamma_{As(V)}$.

$\Gamma_{As(V)}$ depends also on pH (Fig. 7). The shape of the observed trend, which exhibits a marked change in slope at pH ≈ pQ_{a3}, resembles the pH adsorption envelopes of chemisorbing anions [33,36].

The different affinities of chromate and arsenate for the edges of Cl-hydrotalcite are also reflected in the unlike electrophoretic behavior of the particles (Fig. 8). The ζ vs. pH profile of Cl-hydrotalcite suspended in KCl is typical of solids bearing both permanent and variable charges; after all, LDHs are the positive analogs of clays. The overall surface charge of hydrotalcite ($-\sigma_d$) is thus the result of the contributions due to the basal outer surfaces and the amphoteric edges (Eqs. (9)–(12)), screened by counterion adsorption. The apparent *iep* (Fig. 8) is in reasonable agreement with earlier reports [16] and with the reported *pzc* (~12.1) [37]. Nonetheless, the possible effect of the compression of the electrical double layer on the ζ potential values measured beyond pH 12 should not be ignored.

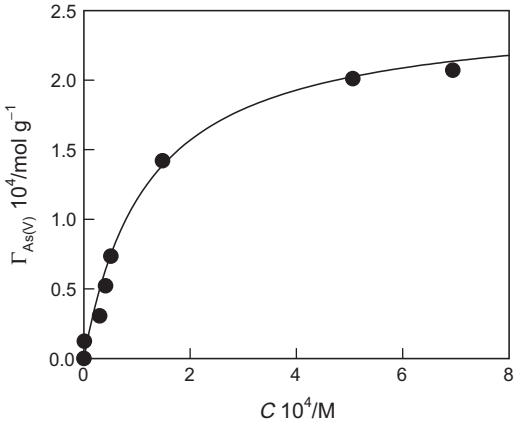

Fig. 6. As(V) edge excess as a function of the arsenate equilibrium concentration; added KCl concentration: 0.3 M; hydrotalcite load: 0.84 g L^{-1}; pH = 9.3 ± 0.1. The solid line shows the fit to the Langmuir adsorption isotherm.

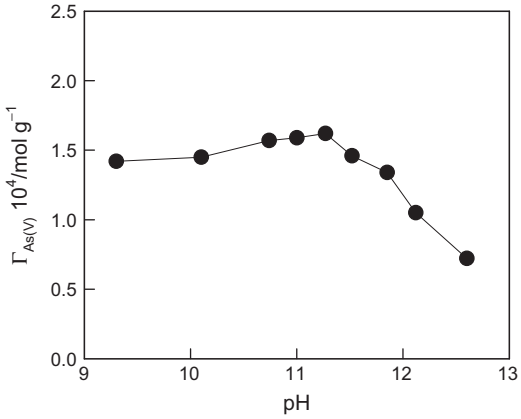

Fig. 7. As(V) edge excess as a function of pH; total As(V) concentration: 2.7×10^{-4} M; added KCl concentration: 0.3 M; hydrotalcite load: 0.84 g L^{-1}. The solid line is a guide to the eye.

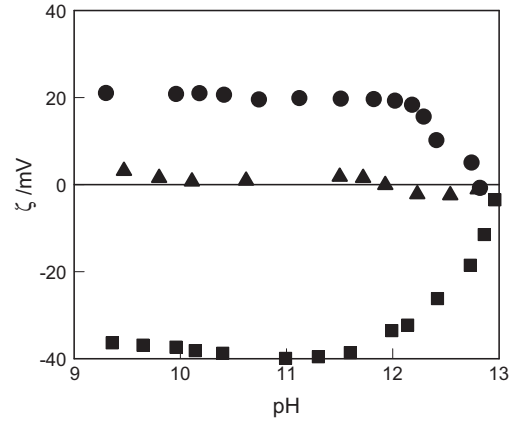

Fig. 8. pH dependence of the ζ-potential of hydrotalcite immersed in (●) 5×10^{-3} M KCl, (▲) 5×10^{-3} M K_2CrO_4, and (■) 5×10^{-3} M Na_2HAsO_4.

$$\equiv Mg(OH)(OH_2) + H^+ \rightleftarrows \equiv Mg(OH_2)(OH_2)^+ \quad (9)$$

$$\equiv Mg(OH)(OH_2) \rightleftarrows \equiv Mg(OH)(OH)^- + H^+ \quad (10)$$

$$\equiv Al(OH)(OH_2) + H^+ \rightleftarrows \equiv Al(OH_2)(OH_2)^+ \quad (11)$$

$$\equiv Al(OH)(OH_2) \rightleftarrows \equiv Al(OH)(OH)^- + H^+ \quad (12)$$

In the presence of CrO_4^{2-}, ζ drops dramatically (Fig. 8), indicating that the positive charge of the basal surfaces and of the edge sites is counterbalanced almost completely. Whether the faint *iep* observed around pH 11.9 reflects the contribution of a minor amount of chromate inner-sphere edge complexes is an open question; ζ potential values are strongly sensitive toward subtle changes of surface speciation [38]. The effect of $HAsO_4^{2-}$ on the electrophoretic behavior of hydrotalcite is even more marked (Fig. 8). Arsenate reverses the charge of the particles in the entire pH range, a fact that can solely be attributed to the formation of negatively charged in-

ner-sphere edge complexes (Eqs. (5) and (6)). Importantly, the observed ζ vs. pH profile mirrors the pH dependency of $\Gamma_{As(V)}$ (Fig. 7), and the absolute value of ζ decreases as arsenate desorbs.

A detailed description of the distribution of charge and potential across the hydrotalcite/aqueous solution interface is beyond the purpose of this study; the ideas behind the modeling of the charging of laminar solids can be found elsewhere [39–42].

The ideas discussed here are in line with the earlier suggestion of Goh et al. [16], who anticipated the role of inner-sphere surface complexation in the uptake of oxyanions by hydrotalcite. It is fair mentioning, however, that they reported a significantly lesser influence of $NaNO_3$ on the uptake of chromate. Surprisingly, they also reported that chromate produced a slight decrease in the ζ potential of the particles, with a small shift in the *iep*. These results are at variance with those presented here. Despite the source of these discrepancies is unclear, the consistency of all our own results is remarkable. Furthermore, they are sound proof of the role played by edge sites.

4. Conclusions

In summary, this work demonstrates that surface sites at the edges of hydrotalcite particles are prone to form inner-sphere edge complexes with dissolved anionic ligands. Complexation at edges is a particular case of the widely accepted surface complexation approach, its underlying concepts accounting well for the different affinities of chromate and arsenate.

Manifestation of chemisorption on edge sites depends not only on affinity, but also on particle size, because the latter determines the number of edge sites per mole of hydrotalcite. For small, nano-sized, platelets, the contribution of edge complexation to the overall anion removal should be noticeable and increasingly important as particle size reduces. For larger particles, say in the micron-size range, the number of edge sites reduces significantly, and their role in anion uptake becomes silent; viz. the maximum uptake shall be solely determined by the stoichiometries of the LDH and the anion exchange reaction. Notwithstanding, the role of edges have not been perceived in the previous studies of chromate and arsenate removal by LDHs.

Acknowledgments

This work was partially supported by ANPCyT (PICT 06-06631) and CONICET (PIP 4196). MJ and AER are members of CONICET.

Appendix A. Supplementary material

Supplementary data associated with this article can be found, in the online version, at http://dx.doi.org/10.1016/j.jcis.2012.10.069.

References

[1] A. Vaccari, Appl. Clay Sci. 14 (1999) 161–198.
[2] S. Carlino, Solid State Ionics 98 (1997) 73–84.
[3] V. Rives, M.A. Ulibarri, Coord. Chem. Rev. 181 (1999) 61–120.
[4] A. Ookubo, K. Ooi, F. Tani, H. Hayashi, Langmuir 10 (1994) 407–411.
[5] L.M. Parker, N.B. Milestone, R.H. Newman, Ind. Eng. Chem. Res. 34 (1995) 1196–1202.
[6] J. Das, D. Das, G.P. Dash, K.M. Parida, J. Colloid Interface Sci. 251 (2002) 26–32.
[7] D. Das, J. Das, K.M. Parida, J. Colloid Interface Sci. 261 (2003) 213–220.
[8] L. Yang, Z. Shahrivari, P.K.T. Liu, M. Sahimi, T.T. Tsotsis, Ind. Eng. Chem. Res. 44 (2005) 6804–6815.
[9] S.V. Prasanna, R.A.P. Rao, P.V. Kamath, J. Colloid Interface Sci. 304 (2006) 292–299.
[10] K.-H. Goh, T.-T. Lim, Z. Dong, Water Res. 42 (2008) 1343–1368.
[11] X.-Y. Yu, T. Luo, Y. Jia, R.-X. Xu, C. Gao, Y.-X. Zhang, J.-H. Liu, X.-J. Huang, Nanoscale 4 (2012) 3466–3474.
[12] S. Miyata, Clays Clay Miner. 31 (1983) 305–311.
[13] Y. Israëli, C. Taviot-Guého, J.-P. Besse, J.-P. Morel, N. Morel-Desrosiers, Dalton (2000) 791–796.
[14] N. Morel-Desrosiers, J. Pisson, Y. Israëli, C. Taviot-Guého, J.-P. Besse, J.-P. Morel, J. Mater. Chem. 13 (2003) 2582–2585.
[15] Y. Wang, H. Gao, J. Colloid Interface Sci. 301 (2006) 19–26.
[16] K.-H. Goh, T.-T. Lim, A. Banas, Z. Dong, J. Hazard. Mater. 179 (2010) 818–827.
[17] D.A. Dzombak, F.M.M. Morel, Surface Complexation Modeling, John Wiley and Sons, New York, 1990.
[18] W. Stumm, Chemistry of the Solid–Water Interface, Wiley-Interscience, New York, 1992.
[19] M.A. Blesa, P.J. Morando, A.E. Regazzoni, Chemical Dissolution of Metal Oxides, CRC Press, Boca Raton, Fla., USA, 1994.
[20] M. Jobbágy, A.E. Regazzoni, J. Phys. Chem. B 109 (2005) 389–393.
[21] M. Jobbágy, A.E. Regazzoni, Appl. Clay Sci. 51 (2011) 366–369.
[22] G. Bascialla, A.E. Regazzoni, Colloids Surf. A 328 (2008) 34–39.
[23] A.M. Fogg, J.S. Dunn, D. O'Hare, Chem. Mater. 10 (1998) 356–360.
[24] F. Millange, R.I. Walton, L. Lei, D. O'Hare, Chem. Mater. 12 (2000) 1990–1994.
[25] N. Iyi, K. Kurashima, T. Fujita, Chem. Mater. 14 (2002) 583–589.
[26] T. Hiemstra, W.H. Van Riemsdijk, G.H. Bolt, J. Colloid Interface Sci. 133 (1989) 91–104.
[27] T. Hiemstra, J. Colloid Interface Sci. 133 (1989) 105–117.
[28] T. Hiemstra, W.H. Van Riemsdijk, J. Colloid Interface Sci. 301 (2006) 1–18.
[29] R. Rodríguez, M.A. Blesa, A.E. Regazzoni, J. Colloid Interface Sci. 177 (1996) 122–131.
[30] J. Rosenqvist, W.H. Casey, Geochim. Cosmochim. Acta 68 (2004) 3547–3555.
[31] S.R. Randall, D.M. Sherman, K.V. Ragnarsdottir, Geochim. Cosmochim. Acta 65 (2001) 1015–1023.
[32] S. Fendorf, M.J. Eick, P. Grossl, D.L. Sparks, Environ. Sci. Technol. 31 (1997) 315–320.
[33] M.A. Anderson, J.F. Ferguson, J. Gavis, J. Colloid Interface Sci. 54 (1976) 391–399.
[34] Y. Arai, E.J. Elzinga, D.L. Sparks, J. Colloid Interface Sci. 235 (2001) 80–88.
[35] S. Goldberg, C.T. Johnston, J. Colloid Interface Sci. 234 (2001) 204–216.
[36] F.J. Hingston, R.J. Atkinson, A.M. Posner, J.P. Quirk, Nature 215 (1967) 1459–1461.
[37] S. Han, W. Hou, C. Zhang, D. Sun, X. Huang, G. Wang, J. Chem. Faraday Trans. 94 (1998) 915–918.
[38] M.A. Blesa, A.J.G. Maroto, A.E. Regazzoni, J. Colloid Interface Sci. 99 (1984) 32–40.
[39] M.J. Avena, C.P. De Pauli, J. Colloid Interface Sci. 202 (1998) 195–204.
[40] I.C. Bourg, G. Sposito, A.C.M. Bourg, J. Colloid Interface Sci. 312 (2007) 297–310.
[41] R. Rojas-Delgado, M. Arandigoyen-Vidaurre, C.P. De Pauli, M.A. Ulibarri, M.J. Avena, J. Colloid Interface Sci. 280 (2004) 431–441.
[42] A. Mercado, E.M. Farfán-Torres, A.E. Regazzoni, M.A. Blesa, Colloids Surf. A 218 (2003) 277–284.